

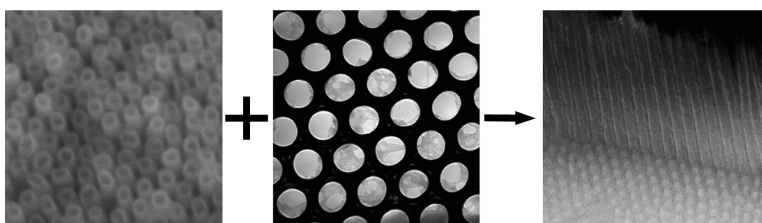
Communication

## As a Whole: Crystalline Zinc Aluminate Nanotube Array–Nanonet

Yu Wang, and Kai Wu

*J. Am. Chem. Soc.*, **2005**, 127 (27), 9686-9687 • DOI: 10.1021/ja0505402 • Publication Date (Web): 15 June 2005

Downloaded from <http://pubs.acs.org> on March 25, 2009



### More About This Article

Additional resources and features associated with this article are available within the HTML version:

- Supporting Information
- Links to the 14 articles that cite this article, as of the time of this article download
- Access to high resolution figures
- Links to articles and content related to this article
- Copyright permission to reproduce figures and/or text from this article

[View the Full Text HTML](#)



## As a Whole: Crystalline Zinc Aluminate Nanotube Array–Nanonet

Yu Wang and Kai Wu\*

State Key Laboratory for Structural Chemistry of Unstable and Stable Species, Institute of Physical Chemistry, College of Chemistry and Molecular Engineering, Peking University, Beijing 100871, China

Received January 27, 2005; E-mail: kaiwu@pku.edu.cn.

Controlled growth of nanostructures is of great importance in nanoscience and technology and is one of the main concerns for researchers. In all approaches employed, template-assisted synthesis of nanomaterials turns out to be quite effective.<sup>1</sup> In particular, an anodized aluminum oxide (AAO) template is very useful in fabrication of hierarchically ordered structures because its structural parameters can be feasibly controlled by tuning its anodization conditions.<sup>2</sup> The AAO template has both external and internal surfaces that can be utilized. For instance, its internal surfaces have been successfully utilized to prepare carbon nanotube (CNT) arrays<sup>3</sup> and further used the prepared CNTs in pores as a secondary template to routinely prepare uniform metal nanotubes by a replication method.<sup>4</sup>

Here, we exploit both the AAO external and internal surfaces to prepare a complex, but with ordered crystalline structure: integrated zinc aluminate nanotube array sitting on its nanonet. This array/net complex structure exists as a whole.

Zinc aluminate ( $\text{ZnAl}_2\text{O}_4$ ), often referred as zinc spinel, is a useful material. It mainly serves as catalysts and catalyst supports in synthesis, dehydrogenation, dehydrocyclization, hydrogenation, dehydration, isomerization, and combustion processes.<sup>5</sup> It is a wide band-gap semiconductor (3.8 eV)<sup>6</sup> that can be used as a transparent conductor,<sup>7</sup> a dielectric,<sup>8</sup> or optical materials.<sup>6a,9</sup> Recently, much attention has been paid to the luminescence properties of rare-earth doped zinc spinels.<sup>10</sup> To prepare  $\text{ZnAl}_2\text{O}_4$ , people have employed various synthesis approaches using either solid ZnO and  $\alpha\text{-Al}_2\text{O}_3$  or Al- and Zn-containing complexes as precursors, normally yielding small porous crystallites.<sup>9–11</sup>

In this study, a laboratory-prepared AAO template (by two-step anodization in oxalic acid<sup>3</sup>) was buried in pure ZnO powder ( $0.6 \pm 0.4 \mu\text{m}$  in particle size) pretreated with alcohol. Then the AAO template in the slurry ZnO was sonicated for 5–10 min before being placed into a Muffle furnace. The furnace temperature was then slowly increased to 650 °C in air and remained for 5 h before cooling down to room temperature (RT). The as-treated AAO template was then buried in fresh ZnO powder, again, in a quartz boat that was then sent into a chemical-vapor deposition (CVD) device. Afterward, the CVD temperature was increased to 650 °C at 10 °C/min in a high purity  $\text{N}_2$  flow of 30 sccm at 1 atm. After 30 min, the temperature further increased to 680 °C at about 1 °C/min, and the gas flow was swapped to 30 sccm  $\text{H}_2$  (1 atm). The sample was kept in the CVD device for > 16 h. Finally, the sample was cooled to RT in  $\text{N}_2$  flow. For further analyses, concentrated HF acid was used to remove the AAO template. The morphology and structure of the prepared samples were analyzed by a scanning electron microscope (SEM, Strata DB235, FEI), environmental SEM (ESEM, Quanta 200F, FEI), a transmission electron microscope (TEM, JEM 200 CX JEOL), high-resolution TEM (HRTEM, Tecnai F30, Philips), and X-ray diffraction (XRD, Rigaku D/MAX-200 X-ray powder diffractometer).

Figure 1 shows the morphology of the prepared sample (AAO template already removed). According to Figure 1a, the free-

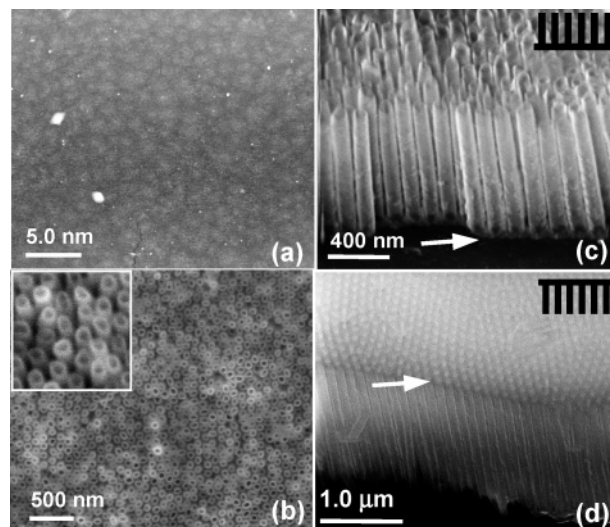


**Figure 1.** (a) Large-scale and (b) enlarged ESEM images of the sample (AAO template removed). Inset in (b) is a close-up of the tubes. SEM side view images of the samples in (c) upside and (d) upside-down positions. The drawings in (c) and (d) show the tube orientations. Arrows in (c) and (d) indicate the positions of the thin holed layer.

standing sample area was about  $30 \mu\text{m} \times 30 \mu\text{m}$ . A top view (Figure 1b and its inset) revealed that open-ended nanotubes of  $\sim 80 \text{ nm}$  in diameter and  $\sim 15 \text{ nm}$  in wall thickness indeed formed. A side view (Figure 1c) demonstrated that the tubes were about 800 nm in length and sit on a thin layer that has some holes (as indicated by the arrow). If it is upside down (Figure 1d), one could clearly identify the pores in the thin layer (as pointed out by the arrow). This thin layer was very similar to the AAO template in surface morphology. From the thin layer side, TEM (Figure 2a) clearly showed the nanonet structure: pores in hexagonal packing. The inner diameter of each pore was  $\sim 75 \text{ nm}$  and the spacing between two neighboring pores  $\sim 25 \text{ nm}$ . Selected area electron diffraction (SEAD, inset in Figure 2a) substantiated that the nanonet was a crystal with a structure very similar to that for face-centered cubic (FCC)  $\text{ZnAl}_2\text{O}_4$ , and grew along the  $[\bar{1}12]$  direction. From the nanotube side (Figure 2b), each tube sits on an underlying pore and the tube wall thickness was  $\sim 15 \text{ nm}$ .

To uncover the details of the crystal structure, HRTEM measurements were taken in the 3-fold hollow area and near the tube edge (the triangle and circle areas in Figure 2b, respectively). In the hollow area (Figure 2c), a rectangular lattice structure was displayed, one side being 0.46 nm and the other 0.28 nm. Near the tube edge (Figure 1d) appeared the same lattice structure, meaning that the tube structure is identical to the nanonet structure. Note that near the tube edge (as indicated by the long black arrow in Figure 2d) the lattice on the tube wall surface well matched that of the tube tip surface. To further verify the crystal structure, XRD measurement was taken for the as-prepared sample (with the AAO template intact, otherwise it was too thin to use). The spectrum (Figure 2e)

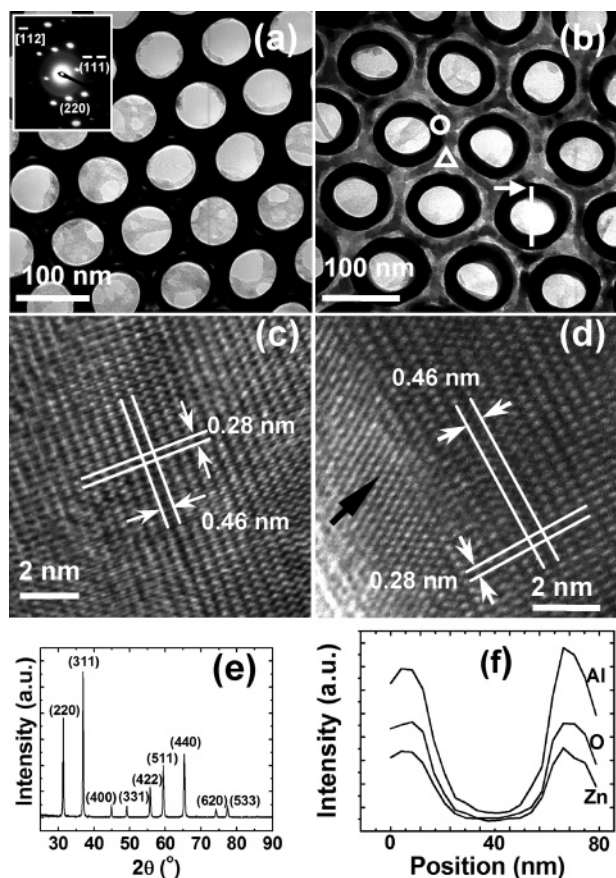
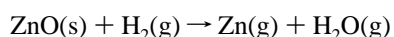


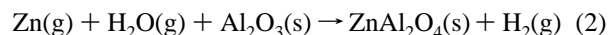
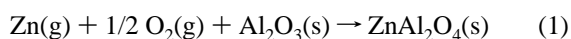
**Figure 2.** TEM images of the nanotube array plus nanonet structure viewed from (a) the nanonet side and (b) the tube side. Inset in (a) is the SEAD pattern from (a). Panels (c) and (d) are HRTEM images showing the lattice structures near a tube top-edge [the circle in (b)] and in the three-fold hollow area [the triangle in (b)], respectively. Panel (e) is an XRD spectrum of the sample with the AAO template intact. Panel (f) is an EDX profile scanned along the line across a tube in the tube array in (b). The arrow in (b) indicates the starting point of the line-scan.

again showed that there existed solely  $\text{ZnAl}_2\text{O}_4$  crystallites in the sample. Local composition EDX spectrum (Figure 2f) was collected along the line across a nanotube in Figure 2b. The line scan analysis (after sensitivity calibration) unambiguously showed that the stoichiometric atom concentration ratio was  $\text{Zn}:\text{Al}:\text{O} \approx 13.8:31.6:54.6\% \approx 1:2:4$ . Obviously, the obtained materials were crystalline  $\text{ZnAl}_2\text{O}_4$ . The thickness of the tube wall or net was thinner than 20 nm.

One possible growth mechanism is proposed in tandem with our experimental observations and measurements. Pretreatment of AAO and ZnO in alcohol served two aims: preventing the AAO backbone structure from collapsing at elevated temperatures and modifying the surfaces of the AAO template and the ZnO particles. In CVD, Zn vapor was formed by reduction of ZnO with  $\text{H}_2$  (the reaction free energy change becomes negative, about  $-40$  kJ/mol, under our experimental conditions):



Zn vapor further reacted with AAO to form  $\text{ZnAl}_2\text{O}_4$  at the presence of residual oxygen or formed water via either of the following reactions:



The above judgment is supported by the fact that no  $\text{ZnAl}_2\text{O}_4$  nanotube/nanonet structure was formed under our experimental conditions without  $\text{H}_2$  reduction. During the long growth time, crystallization went on and overtook vaporization at the AAO surfaces so long as a suitable Zn vapor pressure was maintained. This led to crystalline  $\text{ZnAl}_2\text{O}_4$  formation. Our experimentally measured growth kinetics showed that the maximum thickness of the  $\text{ZnAl}_2\text{O}_4$  nanotube wall or nanonet could not be larger than 20 nm under the experimental conditions, implying that the in situ produced Zn vapor could not go very deep into bulk AAO, and hence, the reaction could only occur in the AAO surface regions. Therefore, the reaction is diffusion-limited.

In summary, the crystalline  $\text{ZnAl}_2\text{O}_4$  nanotube array and nanonet have been successfully prepared. These two structures seamlessly join as a whole. This integrated crystalline  $\text{ZnAl}_2\text{O}_4$  structure may be useful in cathodoluminescence, photonics, catalysis, and field emission. The used approach may also be applied to synthesize other useful inorganic nanotube array/nanonets.

**Acknowledgment.** This work is jointly supported by NSFC (20125309, 90206012, 20433010), NKBRF (G2000077503), RFDP of the Ministry of Education of China.

**Supporting Information Available:** The growth kinetics of the  $\text{ZnAl}_2\text{O}_4$  nanotube/nanonet and the effect of alcohol pretreatment. This material is available free of charge via the Internet at <http://pubs.acs.org>.

## References

- Hulteen, J. C.; Martin, C. R. *J. Mater. Chem.* **1997**, *7*, 1075–1087.
- Sulka, G. D.; Stroobants, S.; Moshchalkov, V.; Borghs, G.; Celis, J.-P. *J. Electrochem. Soc.* **2002**, *149*, D97–D103.
- Gao, H.; Mu, C.; Wang, F.; Xu, D. S.; Wu, K.; Xie, Y. C.; Liu, S.; Wang, E. G.; Xu, J.; Yu, D. P. *J. Appl. Phys.* **2003**, *93*, 5602–5605.
- Mu, C.; Yu, Y. X.; Wang, R. M.; Wu, K.; Xu, D. S. *Adv. Mater.* **2004**, *16*, 1550–1553.
- (a) Le Peltier, F.; Chaumette, P.; Saussey, J.; Bettahar, M. M.; Lavalley, J. C. *J. Mol. Catal. A* **1997**, *122*, 131–139. (b) Kinnemann, A.; Idriss, H.; Hindermann, J. P.; Lavalley, J. C.; Vallet, A.; Chaumette, P.; Coutry, Ph. *Appl. Catal.* **1990**, *59*, 165–184. (c) Bart, J. C. J.; Sneeden, R. P. A. *Catal. Today* **1987**, *2*, 1–124. (d) Kienle, C.; Schinzer, C.; Lentmaier, J.; Schaal, O.; Kemmlersack, S. *Mater. Chem. Phys.* **1997**, *49*, 211–216. (e) Valenzuela, M. A.; Aguilar, A.; Bosch, P.; Armendariz, H.; Salas, P.; Montoya, A. *Catal. Lett.* **1992**, *15*, 179–188. (f) Valenzuela, M. A.; Bosch, P.; Aguilar-Rios, G.; Zapata, B.; Maldonado, C.; Schifer, I. *J. Mol. Catal.* **1993**, *84*, 177–186. (g) Roesky, R.; Weiguny, J.; Bestgen, H.; Dingerdissen, U. *Appl. Catal. A* **1999**, *176*, 213–220. (h) Wrzyszczyk, J.; Zawadzki, M.; Trawczyński, J.; Grabowska, H.; Mišta, W. *Appl. Catal. A* **2001**, *210*, 263–269.
- (a) Sampath, S. K.; Cordaro, J. F. *J. Am. Ceram. Soc.* **1998**, *81*, 649–654. (b) Sampath, S. K.; Kanhere, D. G.; Pandey, R. J. *Phys. Condens. Matter* **1999**, *11*, 3635–3644.
- García-Hipólito, M.; Guzmán-Mendoza, J.; Martínez, E.; Alvarez-Fregoso, O.; Falcony, C. *Phys. Status Solidi A* **2004**, *201*, 1510–1517.
- van der Laag, N. J.; Snel, M. D.; Magusin, P. C. M. M.; de With, G. J. *Eur. Ceram. Soc.* **2004**, *24*, 2417–2424.
- Mathur, S.; Veith, M.; Haas, M.; Shen, H.; Lecerf, N.; Huch, V. *J. Am. Ceram. Soc.* **2001**, *84*, 1921–1928.
- (a) Streck, W.; Deren, P.; Bednarkiewicz, A.; Zawadzki, M.; Wrzyszczyk, J. *J. Alloys Compd.* **2000**, *300–301*, 456–458. (b) Zawadzki, M.; Wrzyszczyk, J.; Streck, W.; Hreniak, D. *J. Alloys Compd.* **2001**, *323–324*, 279–282. (c) García-Hipólito, M.; Corona-Ocampo, A.; Alvarez-Fregoso, O.; Martínez, E.; Guzmán-Mendoza, J.; Falcony, C. *Phys. Status Solidi A* **2004**, *201*, 72–79. (d) García-Hipólito, M.; Hernández-Pérez, C. D.; Alvarez-Fregoso, O.; Martínez, E.; Guzmán-Mendoza, J.; Falcony, C. *Opt. Mater.* **2003**, *22*, 345–351. (e) Lou, Z.; Hao, J. *Thin Solid Films* **2004**, *450*, 334–340.
- (a) Valenzuela, M. A.; Jacobs, J.-P.; Bosch, P.; Reijne, S.; Zapata, B.; Brongersma, H. H. *Appl. Catal. A* **1997**, *148*, 315–324. (b) Zawadzki, M.; Wrzyszczyk, J. *Mater. Res. Bull.* **2000**, *35*, 109–114. (c) Fang, C. M.; Loong, C.-K.; de Wijs, G. A.; de With, G. *Phys. Rev. B* **2002**, *66*, 144301. (d) Chen, L.; Sun, X.; Liu, Y.; Zhou, K.; Li, Y. *J. Alloys Compd.* **2004**, *376*, 257–261. (e) Chen, Z.; Shi, E.; Li, W.; Zheng, Y.; Wu, N.; Zhong, W. *J. Am. Ceram. Soc.* **2002**, *85*, 2949–2955. (f) Bi, Z.; Zhang, R.; Wang, X.; Gu, S.; Shen, B.; Shi, Y.; Liu, Z.; Zheng, Y. *J. Am. Ceram. Soc.* **2003**, *86*, 2059–2062.

JA0505402